Applied Physics A (2025) 131:985
https://doi.org/10.1007/s00339-025-09139-w

Applied Physics A
Materials Science & Processing

Tunable semiconducting behavior with addition of gallium (Ga)-Boron (B) Dual-doped elements in CdO thin films

Elvan Kiliç[1] · Erman Erdoğan[2]

Received: 17 July 2025 / Accepted: 5 November 2025

Abstract
In this study, CdO thin films with pure and volume ratios of (1.5% and 1.5%) B and Ga separately and dual-doped were coated on ITO substrate using electrodeposition method. Structural, optical and morphological properties of pure, B and Ga dual-doped CdO films coated on ITO were investigated. XRD measurements revealed that the crystal structure of CdO was disrupted and the crystal size decreased in the B and Ga dual-doped CdO films. As a result of optical measurements, it was observed that the optical band gap decreased as the doping ratio increased. As a result of morphological measurements, it was observed that the surface of all film was homogeneous. Spectroscopic ellipsometry was used to determine that the refractive index, extinction coefficient, dielectric constants, and dissipation factor were determined to change with the concentration of B and Ga dual doping. Refractive index values ranged from 0.8 to 2 and extinction coefficient values from 0.05 to 1.2. The dielectric constant values also show significant variation in the visible region.

Keywords CdO thin film · Electrodeposition · Structure · Optical properties · Doped and co-doped CdO

1 Introduction

Semiconductor materials play an important role in modern technology. They have many distinguishing features that set them apart from conductors and insulators, thanks to their superior optical and electrical properties. Semiconductors, which are an important area of research, form the main lines of most technical devices used today. Semiconductors will continue to be relevant in the future due to the direct contribution of research in this field to human life [1]. For years, research has been conducted to make semiconductor technology more useful and effective in other areas. Some research in this field aims to produce new semiconductor materials, while other research aims to determine the electronic properties of these materials and develop new semiconductor circuit elements that utilize these properties. The nanostructure of the circuit elements resulting from research in this field also represents an important milestone for the development of nanotechnology. Metal oxides (ZnO, CdO, TiO_2, SnO_2), which form a different group among semiconductors due to their unique properties, are a class of materials used in the construction of many devices [2, 3].

Thin films are used in many applications such as semiconductor devices, conductive and insulating coatings, etc. for their electrical properties, in reflective and non-reflective coatings, interference filters, etc. for their optical properties, in memory disks for their magnetic properties, and so on [4]. Metal oxide semiconductor films have attracted attention in recent years due to their optical and electrical properties, and research and studies have become increasingly important. One such metal oxide semiconductor is cadmium oxide (CdO).CdO films, which are generally pure and have high electrical conductivity, are n-type semiconductor oxide materials due to the presence of oxygen vacancies or excess cadmium (Cd) atoms as donors. CdO structures are transparent in spectral regions and can be observed with a direct band gap between values. Therefore, pure and doped CdO materials are of great importance due to optoelectronic applications such as supercapacitors [5], photodiodes [6], gas sensors [7] and thin film transistors [8]. The synthesis process and the type of dopant can change the electrical and

✉ Erman Erdoğan
erman.erdogan@bilecik.edu.tr

[1] Department of Physics, Institute of Graduate Studies, Bilecik Seyh Edebali University, Bilecik 11100, Turkey

[2] Department of Electronics and Automation, Vocational High School, Bilecik Seyh Edebali University, Bilecik 11100, Turkey

Published online: 11 November 2025

optical properties. The conductivity and optical properties of CdO films can be observed by doping with various ions. When CdO is synthesized with ions which have an ionic radius smaller than Cd^{+2}, an increase in electrical conductivity and band gap energy is observed.

The efficiency of solar cells and optoelectronic devices can be significantly increased thanks to CdO's structural and optical properties. Doping CdO thin films with metal atoms to create low-resistivity CdO thin films allows for this improvement. Group III elements (B, Al, Ga, and In) are among the metal dopants that are now available; Ga and B elements in particular have drawn possible interest of trivalent cations. Because of its high electronegativity (2.04), several researchers have suggested utilizing boron to investigate the boron effect on the characteristics of CdO thin films. Nonetheless, the optical, morphological, and structural characteristics of the film can be enhanced by concurrently doping the two elements into the host lattice. The synthesis, characterization, and uses of CdO have been extensively studied, including CdO doped with Ga, Al, Se, B, and Dy [9–12]. Co-doping Ga and B with their respective high and low atomic numbers combined has not been studied. With its lowest ionic radius and highest electronegativity, boron is one of the trivalent cations that can most significantly alter the characteristics of CdO thin films. According to certain studies, boron doping provides stable electrical properties and reduces deterioration [13]. Furthermore, due to its higher electronegativity and oxidation resistance, gallium has traditionally been favored for doping CdO thin films [14]. Consequently, the combination of various dopant components may work well to modify the characteristics of CdO thin films. For the first time, our inquiry focuses on the doping of these specific substances. This choice is intended to highlight the work's distinctive originality.

Electrodeposition is an electrochemical process involving the deposition of a film on a substrate by applying an electric current to a solution containing metal ions. In the electrodeposition method, parameters such as the pH value of the solution, temperature, solution additives, growth mode, deposition potential or current density directly affect the quality and properties of the grown coating. It is very important to select these parameters according to the metal coatings to be obtained and to optimize them appropriately. Despite extensive research on doping CdO with single elements such as Ga or B to improve its performance, there remains a significant gap in understanding the effects of co-doping with both Ga and B, particularly regarding their combined impact on the structural, optical, and morphological characteristics of CdO thin films. The main challenges in this area include optimizing the doping process to achieve desired material properties, controlling the insertion and occupation rates of dopants, and developing cost-effective synthesis methods such as electrodeposition that can produce high-quality films for practical applications. These unresolved issues underscore the need for further investigation into co-doping mechanisms to fully harness the potential of CdO-based materials in advanced technological devices. The aim of this study is to investigate the physical properties of the materials produced by using the electrodeposition method to produce low-cost CdO thin films with good physical properties instead of high-cost metal oxides by co-doping Ga and B ions in certain proportions. For this, SEM (Scanning Electron Microscopy), XRD (X-ray diffraction), UV (Ultra Violet Ray) Spectrophotometer, and Spectroscopic Ellipsometry analyses will be performed.

2 Experimental

The chemicals used as coating solution were Cadmium chloride ($CdCl_2 \cdot H_2O$, purity: 99.995%), Sodium hydroxide (NaOH, purity: 99.99%), Ammonium hydroxide (NH_4OH, purity: 99.99%), Gallium nitrate ($Ga(NO_3)_3$, purity: 99.9%), and Boric acid (H_3BO_3, purity: 99.5%) purchased from Sigma-Aldrich. These chemicals have a purity level close to 99%. ITO coated glass and p-Si, (100) surface orientation, shiny on one side and matte on the other, to be used as substrates and their surface resistance values vary between 0 and 10 $\Omega \cdot cm^2$. Before coating, ITO coated glass and p-Si was cut into $1 \times 2 cm^2$ dimensions and then cleaned in an ultrasonic bath for 30 min in deionized water, acetone and isopropanol, respectively. All solutions were prepared with deionized (DI) water. Production was carried out with a three-electrode electrodeposition system. In this system; ITO coated glass and p-Si substrates were used as the working electrode, silver/silver chloride (Ag/AgCl) as the reference electrode, and platinum wire as the counter electrode (Fig. 1).

10 mM ($CdCl_2 \cdot H_2O$), 10mM NaOH, and 1.5% wt. $Ga(NO_3)_3$ and H_3BO_3 were used for the coating solution to fix the pH using NH_4OH value to 10.5. The solution was mixed until a homogeneous electrolyte was formed before production. Production of pure and doped CdO thin films was carried out at room temperature with the chronoamperometry method at a potential of −0.6 V for 1200 s. After the film production was completed, it was immersed in pure water, cleaned, and then dried. Finally, it was annealed in an air at 400 °C for 2 h to form a crystal structure. Surface analyses of the produced films were performed with SEM device (SEM, FESEM FEI Quanta 200 FEG). Crystal structure analysis of the produced thin films was provided using XRD system (PANalytical Xpert Pro MPD, Cu Kα radiation and $\lambda = 1.5418 Å$). Electrochemical analyses were performed

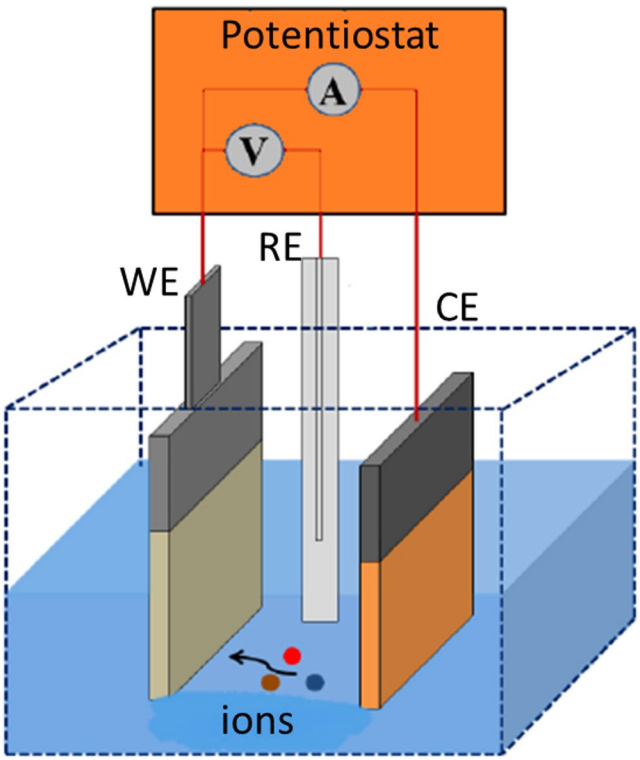

Fig. 1 Schematic representation of the apparatus used in the electrodeposition method

in a controlled manner with the help of Gamry Reference 3000 Potentiostat/Galvanostat system and PH200 electrochemical analysis software. Refractive indices and extinction coefficient were determined using a spectroscopic ellipsometer device. These measurements were carried out in Nigde Omer Halisdemir University Central Laboratory.

3 Results and discussion

3.1 Cyclic voltammetry (CV) and chronoamperometry (CA) analysis

CV is a powerful tool to investigate redox reactions of materials and is performed in a three-electrode electrochemical cell. A potential is applied to the working electrode linearly with a constant scanning speed (V/s) from the initial potential value to the final potential value. The working electrode potential decreases to its original potential at the same rate after reaching the maximum potential. The cyclic scan can be performed repeatedly. To obtain the CV curve, the measured current is plotted against the potential. The voltage-current graph gives specific information to the working electrode immersed in the electrolyte [15].

Chronoamperometry technique is a technique that allows materials to be deposited for a certain period of time and at a constant potential. In order to determine the constant potential, cyclic voltammetry must first be analyzed well (Fig. 2a). As seen in Fig. 2a, there is a current increase in the negative region. This situation is due to ion flow. Therefore, film formation can be mentioned in this region. With the help of cyclic voltammetry technique, the most suitable coating potential of pure and doped CdO thin films was determined as −0.6 V. Then, chronoamperometry technique was used for coating at a constant potential.

As seen in Fig. 2b, the current-time graph of the growth of pure and doped CdO thin films on ITO in 1200 s by applying a potential of −0.6 V is given. The possible reaction for CdO is as follows:

$$CdCl_2 \rightarrow Cd^{2+} + 2Cl^-$$

$$NaOH \rightarrow Na^{2+} + [OH]^{2-}$$

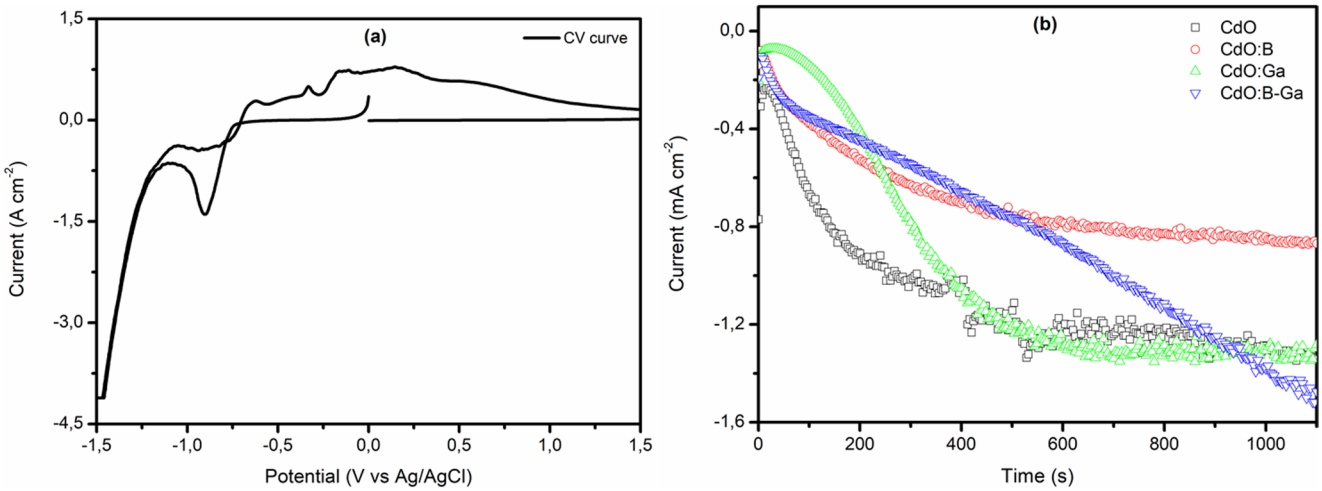

Fig. 2 (**a**) Current-potential (cyclic voltammetry) and (**b**) current-time (chronoamperometry) curves for CdO thin film fabrication

$$CdCl_2 + 2NaOH \rightarrow Cd(OH)_2 + 2NaCl$$

$$CdOH_2 \underrightarrow{annealing} CdO + H_2O$$

The ions in $CdCl_2$ and NaOH used as precursor materials dissociate in aqueous solution and then combine to form $Cd(OH)_2$. In order to obtain the CdO thin film, it is annealed in air and thus the crystal structure is formed. When the chronoamperometry graph given for pure and doped CdO thin films is examined, a high current value is seen due to the rapid ion mobility in the first seconds. At this stage, after the first growth on the ITO coated glass surface, the conductivity value on the electrode surface changes and this situation is reflected as a fixed line in the current curve. The applied time has a serious effect on the film thickness.

The thicknesses of the films were calculated using the gravimetric weight difference method with the formula given below [16]:

$$t = \frac{M_s - M_i}{A.\rho} \quad (1)$$

In this method, first, the ITO substrates were weighed one by one on a precision balance before deposition (M_i), and then re-weighed (M_s) after the film was formed. M_s-M_i gave the weight of the composed film. Here, ρ is the density of the film and A is the surface area of the ITO substrate. When calculating the film thickness, the film was assumed to be of homogeneous thickness and the density value for CdO, boron, and gallium was taken as 8.15 g/cm^3, 2.30 g/cm^3, and 5.90 g/cm^3, respectively. Additionally, to support the thickness results, Faraday's law has been applied to the electrodeposited film by below formula [17]:

$$T = \frac{(JtM)}{(nF\rho)} \quad (2)$$

Here T is the thickness, J is the current density (A/cm^2), t is the deposition time (s), M is the molecular mass (g/mol^1), n is the number of electrons required for the deposition, F is the Faraday constant (96485 C/mole) and ρ is the density (g/cm^3).

The thickness values were found to be 322 nm, 324 nm, 325 nm, and 330 nm for pure CdO, CdO: B, CdO: Ga, and CdO: B-Ga thin films, respectively.

3.2 XRD analysis

The crystal structures of the films were determined using X-ray diffraction analysis. Information about the crystallization of CdO thin films was obtained by looking at the intensity and half-peak width of the peaks from the drawn X-ray graphs. In order to have a good crystallization level in the X-ray diffraction spectrum, there should be peaks with high intensity and narrow half-peak widths on a minimum intensity background. If the half-peak widths are wide and the peak intensities are low, the crystallisation level is said to be low and the material is more irregular. When the diffraction spectra of the CdO thin films obtained in this study were examined, it was seen that there were differences between the peak intensities and widths, and the Miller indices of the relevant planes on the peaks were given with the support of JCPDS card no 05–0640.

X-ray diffraction pattern examination was carried out by scanning in the $20° \leq 2\theta \leq 80°$ angle range at room temperature. The (111), (200), (220), (311) and (222) peaks obtained as a result of the analysis made for the CdO series samples matched the cubic crystal structure. Similar observation for CdO thin film structure was found that the XRD analysis confirmed cubic lattice parameters [18]. The sharp peaks formed show that CdO has good crystallinity. Furthermore, introducing Ga and B to CdO thin films did not change the peak positions of the pure CdO thin film. Examination of the patterns for B and Ga elements reveals that doping does not induce the formation of any new phase in CdO structure (see Fig. 3. (b) and (c)). This observation suggests successful introduction of these atoms into CdO host structure. In addition to the characteristic peaks belonging to pure and doped CdO, the presence of peaks belonging to the OH group can also be mentioned. The diffraction peaks detected at 2θ are related to the diffractions planes as shown in asterix (*) in Fig. 3. (a), corresponding to the monocline symmetry (JCPDS card no. 84–1767) [19].

It has been observed that the peak intensity of the (111) plane in pure CdO thin films gradually decreases with single B and Ga doping. The intensity of the peaks also decreases as a result of B-Ga co-doping, indicating a decrease in crystallinity. This can be attributed to the termination of the crystallisation process due to the co-doping material. This decrease in intensity of the (111) peak is associated with the ionic radii of B^{3+} (0.025 nm) and Ga^{3+} (0.062 nm), which are relatively smaller than that of the host Cd^{2+} (0.097 nm). This suggests effectively incorporating B^{3+} and Ga^{3+} ions into the CdO matrix, occupying the Cd^{2+} sites. A similar phenomenon was observed by M.A.H. Naeem et al. In that research, for Zn-Al co-doped CdO thin films, the preferential orientation was found to shift from (111) to (002) directions at higher doping concentration, meaning that more atoms aligned in this direction at that doping concentration. They reported that the reduction in interatomic spacing occurred as a result of co-doping and also that this phenomenon occurred when smaller ions replaced relatively larger ions [20].

Using the X-ray diffraction results, the crystal sizes and microstrain values of the samples were calculated with the

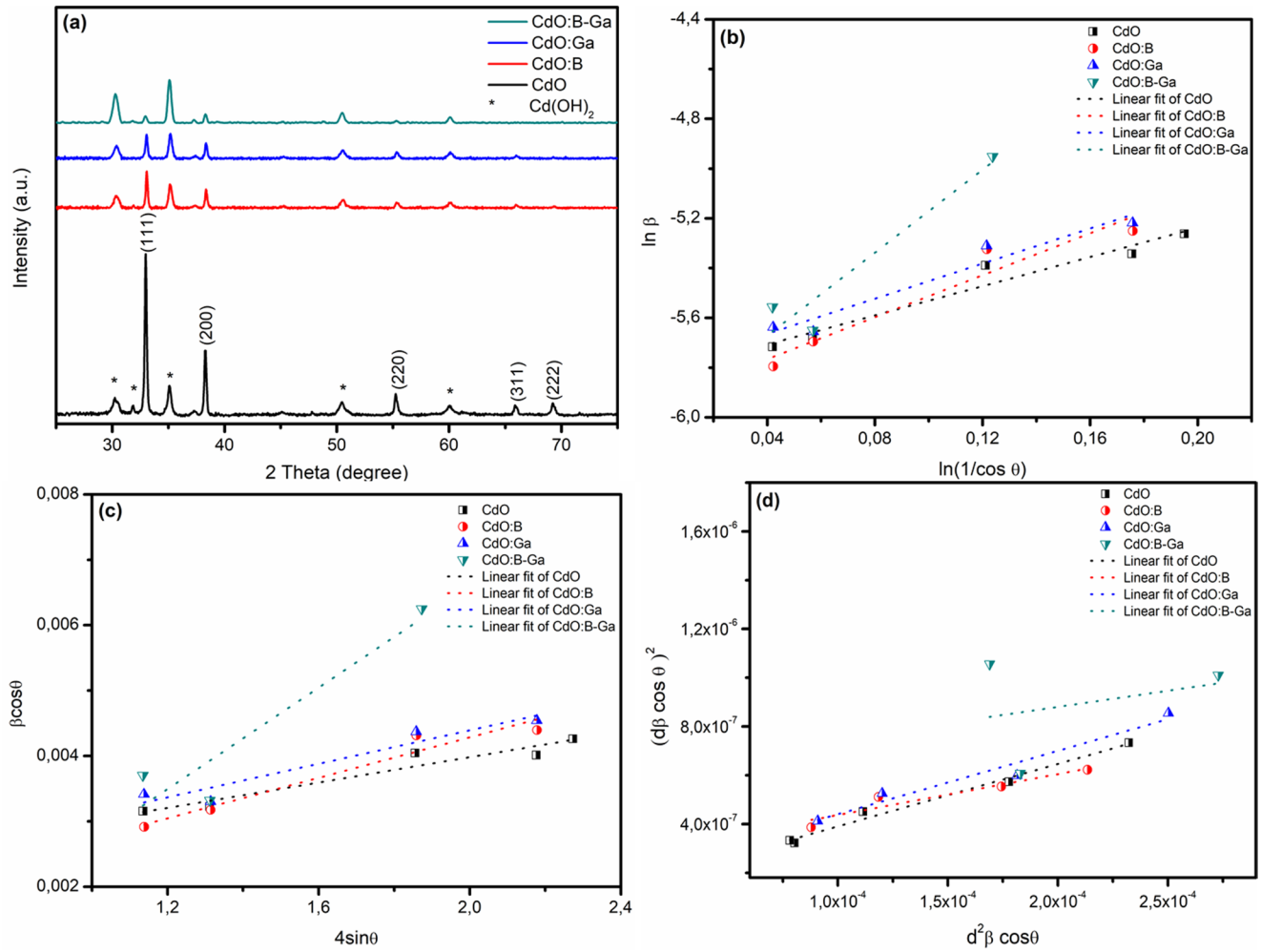

Fig. 3 (**a**) XRD graph (**b**) Modified Scherrer plot (**c**) W-H plot (**d**) SSP plot of pure and doped CdO thin films

help of relations using three different methods. The modified Scherrer equation, which is based on the broadening of diffraction peaks due to size effect can be expressed as below [21], where D represents the size of the crystallite in the direction that is perpendicular to the lattice planes, K is a numerical factor that is commonly known as the crystallite-shape factor, λ is the wavelength of the X-rays, β is the full width at half maximum of the peak (FWHM) of the X-ray diffraction peak in radians, and θ is the Bragg angle.

$$ln\beta = ln\frac{K\lambda}{D} + ln\frac{1}{cos\theta}$$

A straight line with an intercept of around lnK/D and a slope of about one must be obtained if the results of ln versus ln(1/cosθ) are plotted. Using the modified Scherrer equation, the average crystal sizes were found between 46 and 56 nm for all samples and were given in Table 1. Crystal size and microstrain in crystal structures can be calculated with the help of the Williamson-Hall (W-H) Equation given below [22]:

$$\beta\, cos\theta = \frac{K\lambda}{D} + 4\epsilon\, sin\theta$$

Here, β is the FWHM value of the peaks (in radians), θ is the Bragg angle (in radians), K is the dimensionless Scherrer constant, λ is the wavelength of the X-ray source used (in nm), D is the crystal size (in nm) and ϵ is the lattice strain. When the graph is drawn by placing the (4Sinθ) term in the equation above on the x-axis and the (β.Cosθ) term on the y-axis, the best fit line is obtained using the points obtained. Accordingly, the slope of this line gives the micro strain value, while the point where it intersects the y-axis gives information about the average size of the crystals in the sample. By widening the diffraction peak, size-strain parameters can be obtained by taking the mean into account. Using the SSP method in isotropic line broadening makes it easy to obtain average size-strain parameters. Below

Table 1 Comparison of some structural parameters of pure and doped CdO thin films (d_{hkl}: interplanar distance, FWHM: full width half maximum, D_{SR}: crystal size from modified Scherer plot, D_{W-H}: crystal size from WH plot, D_{SSP}: crystal size from SSP plot, ε_{W-H} : microstrain from WH plot, ε_{SSP}: microstrain from SSP plot

	(hkl)	d_{hkl} (Å)	2θ (°)	FWHM(°)	D_{SR} (nm)	D_{W-H} (nm)	D_{SSP} (nm)	ε_{WH} ($x10^{-4}$)	ε_{SSP} ($x10^{-4}$)
CdO	(111)	2.7127	32.98	0.1886	46.93	67.94	78.12	9.7	7.33
	(200)	2.3478	38.29	0.1956					
	(220)	1.6600	55.27	0.2616					
	(311)	1.4151	65.93	0.2740					
	(222)	1.3548	69.27	0.2968					
CdO: B	(111)	2.7055	33.07	0.1743	52.40	77.64	82.41	15.5	10.3
	(200)	2.3437	38.36	0.1926					
	(220)	1.6570	55.38	0.2792					
	(311)	1.4139	65.99	0.3004					
	(222)	-	-	-					
CdO: Ga	(111)	2.7071	33.05	0.2041	46.03	75.73	86.53	12.8	8.50
	(200)	2.3437	38.36	0.2004					
	(220)	1.6575	55.36	0.2830					
	(311)	1.4143	65.97	0.3103					
	(222)	-	-	-					
CdO: B-Ga	(111)	2.7143	32.96	0.2213	56.15	79.65	90.22	38.8	15.6
	(200)	2.3472	38.30	0.2014					
	(220)	1.6444	55.84	0.4052					
	(311)	-	-	-					
	(222)	-	-	-					

equation is approximation to estimate crystallite size and strain values with SSP method [23]:

$$(d_{hkl}\beta_{hkl}cos\theta)^2 = \frac{K}{D}\left(d_{hkl}^2\beta_{hkl}cos\theta\right) + \left(\frac{\epsilon}{2}\right)^2$$

where K is the shape of the particles. The particle size is calculated from the data fitted linearly to the slope and the root of the y-intercept gives the stress. In addition, the slope = Kλ/D, which gives the crystal size. Table 1 shows all the calculated values of average size and strain. It is observed that the crystallite size and strain are consistent in all models. The increase in the estimated strain value is mainly attributed to the contribution of XRD data. The crystallite size estimated using W–H and SSP plots followed the same trend as observed in modified Scherrer's formula. The crystallite size reported using the modified Scherrer formula is smaller than that calculated using other methods. The difference in the estimated crystallite size from the modified Scherrer relation and the size calculated from the W–H and SSP plots is mostly linked to the inclusion of strain in the samples, and the estimated strain values are reasonable.

Pure CdO sample exhibits a crystalline size of 46.93 nm, which decreases to 46.03 nm with an addition of B content and increases to 52.40 nm with an addition of Ga content. This reduction and increment in D value is attributed to the hindering influence of B and Ga atoms on the growth process of CdO thin films. The crystalline size calculated as a result of B and Ga co-doping was found to be larger (56.15 nm). This is thought to be due to the substitutional incorporation between the doping elements and the Cd element in the structure. W. Azzaoui et al. have conducted XRD analysis and the results showed that the CdO crystallite size was not significantly affected by Zn doping and Al-Zn co-doping. The size remained in the range of 21–22 nm [24]. In another study, M.H. Kabir et al. reported that from the XRD analysis, it was confirmed that 3% Ga doped CdO film has not only optimum microstructural properties such as minimum micro strain and dislocation density, but also high crystallinity compared to other Ga doped CdO thin films [25].

3.3 SEM analysis

In a scanning electron microscopy (SEM) image, white and grey areas represent different levels of electron signal intensity. This can provide important information about the composition and topography of the sample. The brightness of areas in the SEM image is influenced by the angle at which the sample's surface reflects electrons. Areas facing the detector directly may appear brighter (white), while areas at steeper angles or shadowed regions appear darker (gray). Differences in atomic number can also affect brightness. Elements with a higher atomic number tend to scatter electrons more effectively, resulting in brighter regions. Conversely, lower atomic number materials scatter electrons less efficiently, appearing darker. In some cases, non-conductive materials can accumulate charge under the electron beam, leading to local brightness variations. Thicker or denser areas of the sample may reflect or scatter more

electrons, appearing brighter compared to thinner or less dense regions.

Figure 4 shows SEM images of pure and doped CdO thin films. Apparently, the CdO thin film (Fig. 4 (a)) shows spherical grains covering the ITO surface with almost the same average size. However, the grains are formed by the clustering of small crystallites on the surface. This results in a topography that is smooth and scattered with fragments and irregular shapes, as well as larger grains. In contrast, when B atoms are incorporated into the CdO structure (Fig. 4 (b)), the spherical grains of the CdO: B thin film are shown to be more clustered and have a less uniform surface coverage. Both small and large grains can be distinguished on the surface, but there is no significant change in the grains observed compared to the pure CdO film. H. Çavuşoğlu et al. investigated how the CdO film surfaces were changed by Co doping and Co: Al dual doping. They reported from SEM photographs that the micro morphologies of the films appeared to be modified with nano-sized particles by adding Co and Al elements to the synthesis solution. In addition, they reported that Co and Al doping played a vital role in shaping the surface of CdO films [26]. Until Ga atoms are incorporated into the CdO structure (Fig. 4(c)), the sample exhibits similarities to the pure CdO sample in terms of grain shape, although the average crystallite size is smaller. Additionally, the distribution of these data shows a higher surface density than that observed in the pure and CdO: B samples. Deokate and Lokhande studied the surface morphology of pure and Ga doped CdO thin films by SEM and reported that they exhibited smooth and regular surface morphology at high Ga doping. At much higher doping ratios, aglamorization of grains was observed by them [27]. As for the dual-doped sample (Fig. 4 (d)), a smooth and dense coating of ITO windows is observed, preserving the spherical grain characteristics. Gallium provides good interconnection throughout the host matrix. In contrast, boron dispersion helps fill the spaces between lattice sites, making the material denser. Knowing that the atomic number of boron (5) is much less than gallium (31), supports the fact

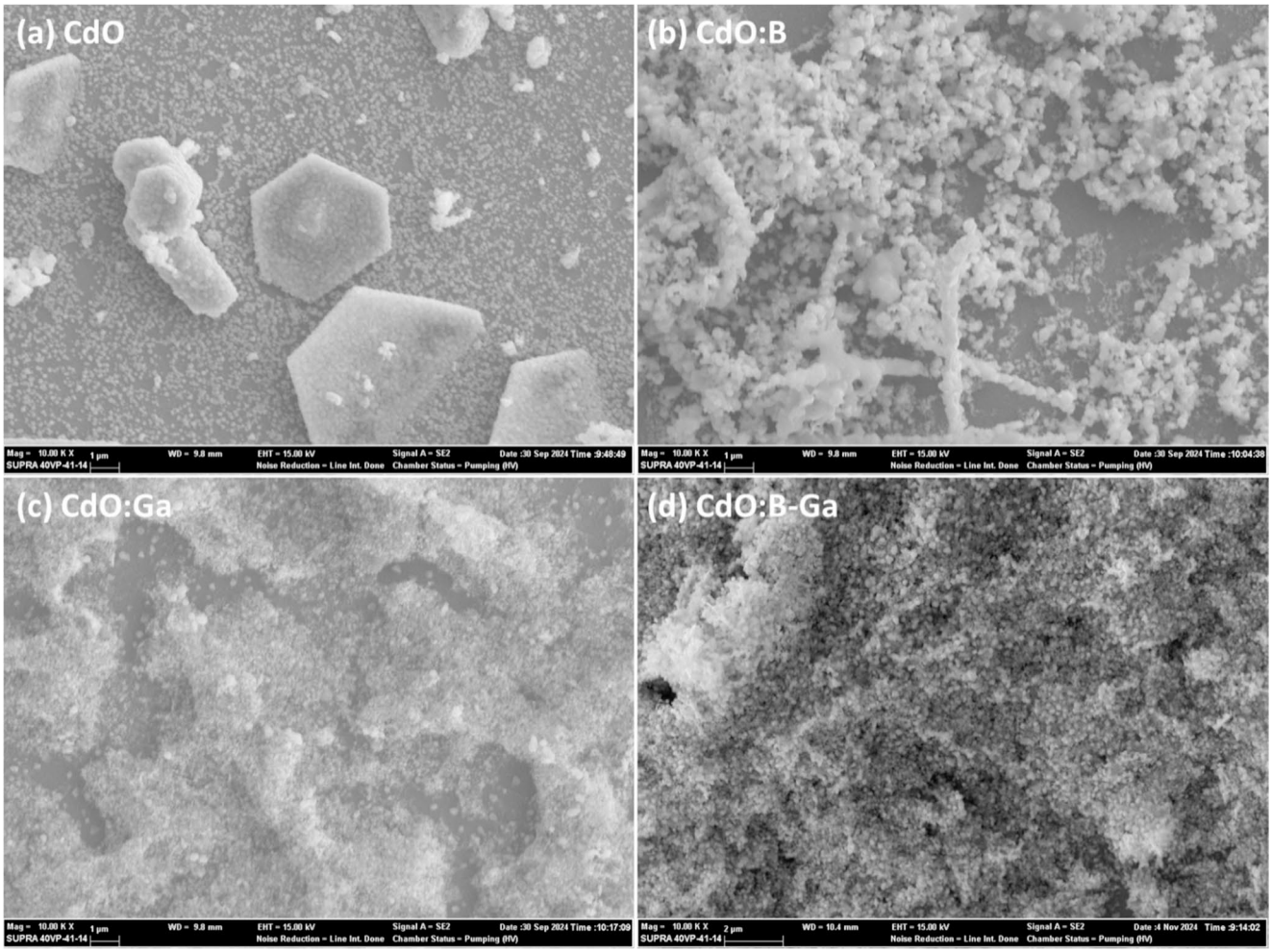

Fig. 4 SEM images of (**a**) pure CdO (**b**) CdO: B (**c**) CdO: Ga (**d**) CdO: B-Ga thin films

that boron is more likely to intercalate into the host matrix of CdO, increasing its final density [28].

EDS measurements were taken for the prepared CdO samples to see whether Cd, O and doped elements were present in the thin films. EDS spectra of pure and doped CdO films are shown in Fig. 5. As can be understood from these images, it shows that the expected elements are present in the thin films and that no other foreign elements are present.

3.4 Optical analysis

When photon energy is sent to the semiconductor, many optical events such as absorption, refraction, reflection, and transmission occur with the interaction of light. In crystalline or amorphous semiconductors, band bending causes narrowing in the energy band gap. The absorbance and transmittance spectra of pure and doped CdO thin films prepared by the electrodeposition method were measured in the wavelength range of 200–900 nm at room temperature. The transmittance spectrum of pure and doped CdO thin films is shown in Fig. 6 (b). It is seen that the transmittance in CdO thin films increases with single doping of B and G. It is seen that the highest transmittance value is reached as a result of co-doping. Transmittance values of around 36%, 48%, 59% and 81% were obtained for the prepared pure CdO, CdO: B, CdO: Ga and CdO: B-Ga thin films in the visible region, respectively. This low transmission for CdO thin film might be attributed to light scattering at the grain boundaries. This notable increase in transmission in CdO thin films upon B and Ga co-doping is likely due to the formation of a smoother surface, as indicated by SEM data. This reduces light scattering, resulting in higher transparency. Similarly, T. Noorunnisha et al. investigated the transmittance spectra of Zn-Co co-doped CdO thin films. The increased transparency was realized for both doped and co-doped films than the pure film. They reported that the higher transmittance realized for co-doped film than the single doped and pure film could be due to the better crystal quality with fewer defects [29].

The absorption spectra of the prepared thin films are given in Fig. 6 (a). When this absorbance graph is examined, a continuous increase is observed at wavelengths of approximately 500 nm. After the wavelength of 500 nm, an equilibrium value of absorption is reached. For this reason, it is seen that the semiconductor material does not absorb at wavelengths greater than 500 nm and therefore it shows transmittance from this value onwards. Strong absorption is shown at wavelengths smaller than 600 nm. The structure obtained as a result of co-doping shows a smaller absorption tendency. This reduction in absorbance could be attributed to lattice structure defect states resulting from differences in

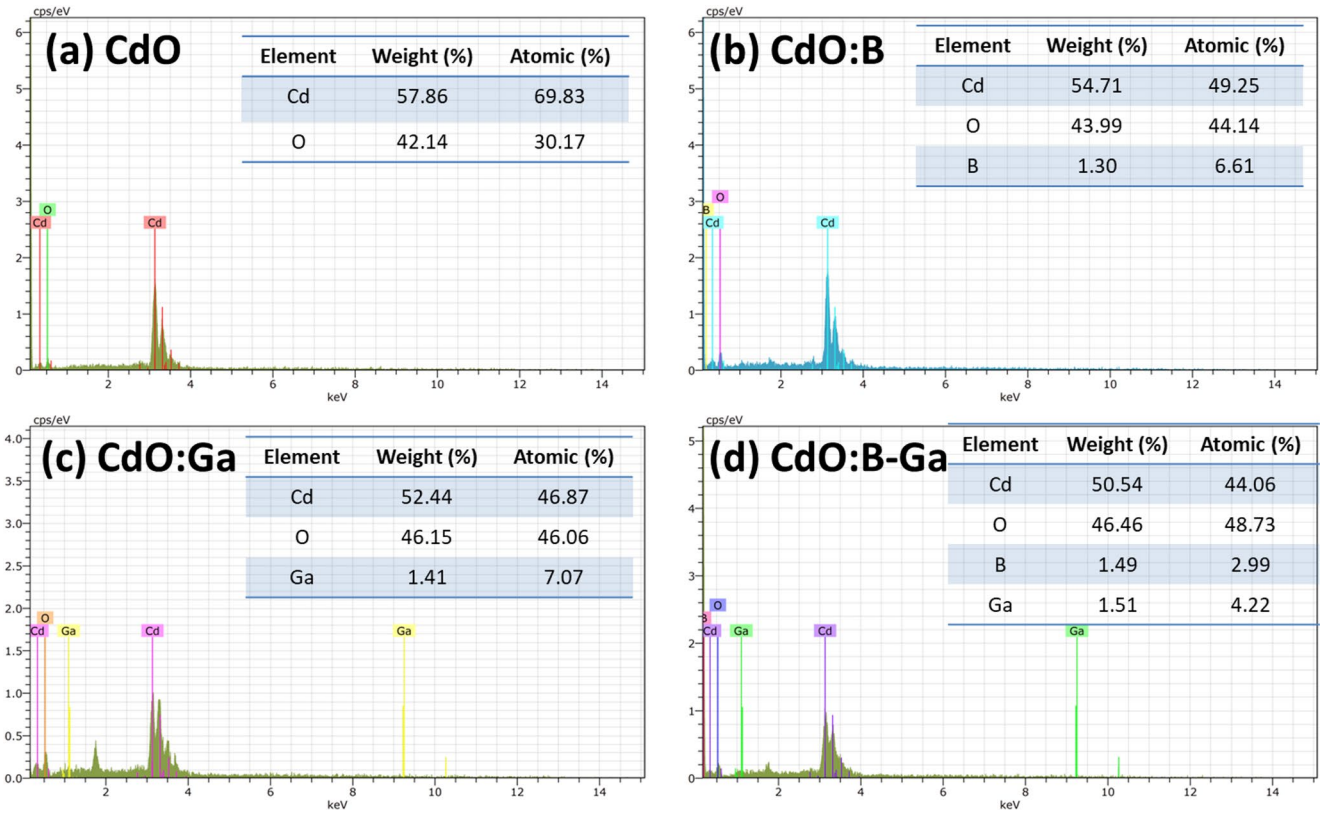

Fig. 5 EDS images of (**a**) pure CdO (**b**) CdO: B (**c**) CdO: Ga (**d**) CdO: B-Ga thin films

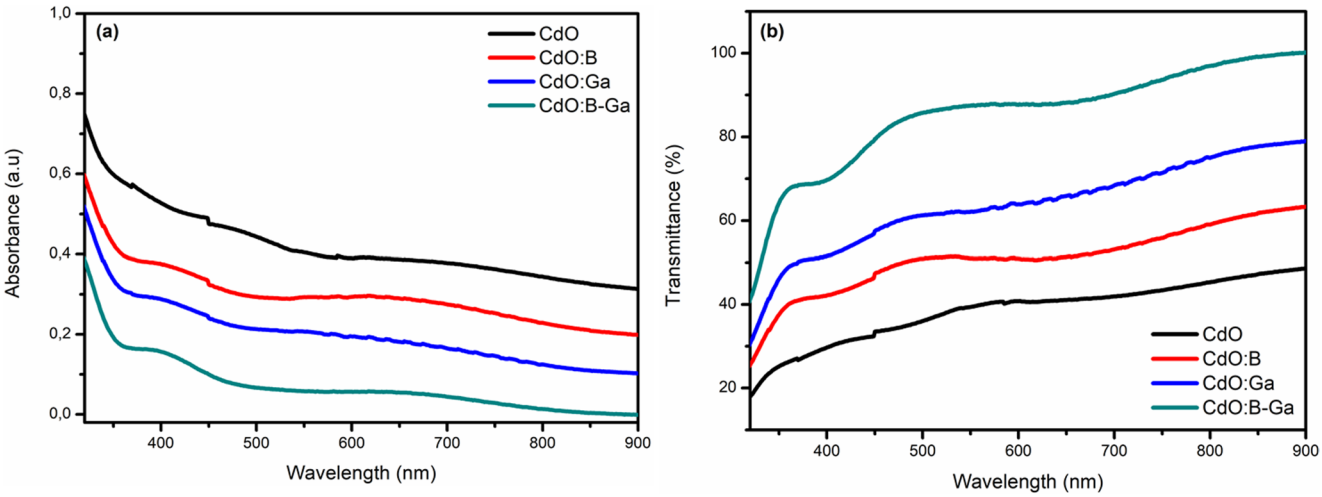

Fig. 6 (**a**) UV-Vis Absorbance graph and (**b**) UV-Vis Transmittance graph of pure and doped CdO thin films

the ionic radii of host and doped elements, as well as light scattering due to grain boundaries. R. Halabi et al. investigated the absorbance spectra of pure and (Mn, Sm) co-doped CdO nanostructures in the UV-visible region. They concluded that all samples showed better absorption in the UV range and less absorption in the visible range [30]. Taking into account the effects of properties such as crystallite size and surface properties on transmittance and absorption graphs, a shift is seen depending on the doping element. It is also seen that these results are compatible with the results of structural and morphological properties and are supported by them.

In the optical analysis of semiconductor thin films, the energy band gaps are determined by using the fundamental absorption spectrum as a result of UV measurements. The relationship between the absorption coefficient and the energy band gap [31]:

$$\alpha\ (h\upsilon\ ) \approx\ (h\upsilon\ -E_g)^n$$

is given by the equation. If both sides of this equation are raised to the 1/nth power,

$$(\alpha\, h\upsilon\ )^{1/n} \approx\ (h\upsilon\ -E_g)$$

the equation is obtained. This relation is used to determine the energy band gap for semiconductors. In the graph drawn against $h\nu$ of $(\alpha h\nu)^{1/n}$, direct transition occurs for $n=1/2$, and indirect transition occurs for $n=2$. Thus, the band type of the semiconductor is determined. The linear regions in these drawn curves are examined. The band type is determined by looking at the value of n from which the most linear region is obtained. In the determined graph, the point where the linear region intersects $h\nu$ at $(\alpha h\nu)^{1/n}=0$ gives the energy band gap.

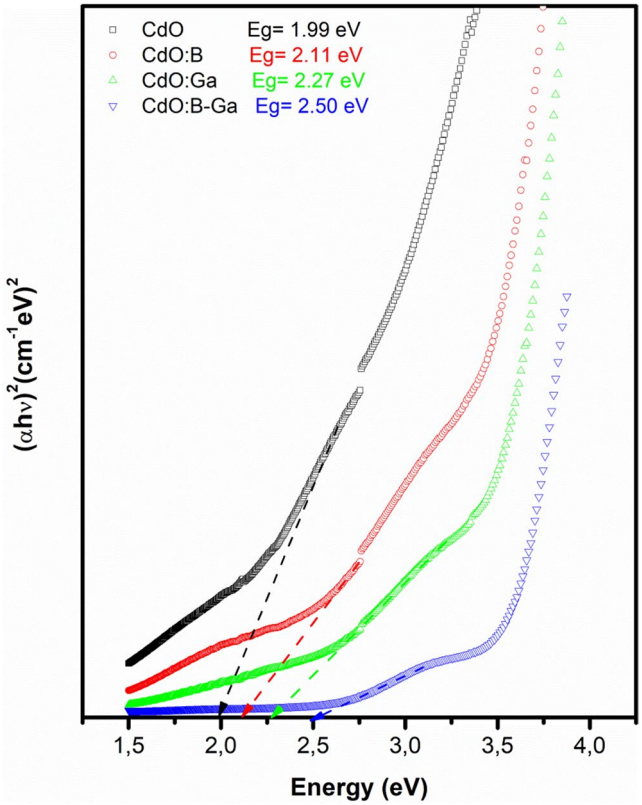

Fig. 7 The Tauc plot of $(\alpha h\nu)^2$ versus hν of pure and doped CdO thin films

As seen in Fig. 7, the E_g values calculated from the $(\alpha h\nu)^2$–$h\nu$ graphs are shown. The graph drawn as a result of the measurements taken shows that the best linearity is that the semiconductor samples have a direct band transition structure. The calculated energy band gaps show that the single and co doping applied to the CdO material causes changes in the energy band gaps of the material. A band gap of 1.99 eV was found in the pure CdO thin film, and

an increasing trend was observed with B, Ga single and B-Ga co-doping, with band gaps of 2.11, 2.27 and 2.50 eV, respectively. The increase in optical band gap energy can be attributed to the quantum confinement effect, which may be caused by replacing Cd elements with B and Ga elements in the CdO lattice structure. This is because the electronegativity and ionic radius of Cd and other dopant elements differ. This band broadening effect can also be explained in terms of the Moss-Burstein effect, where the increased electron density can shift the Fermi energy level to the conduction band edge. The band gap values for all samples suggest potential applications in optoelectronic and photovoltaic devices. Similarly, E. Gürbüz and co-workers investigated the band gap energies of pure, Mn doped and Mn/Ni doped CdO films using the SILAR method. They reported that the Eg value for the pure CdO film was 2.20 eV. It is clear that the optical energy gap for Mn doped CdO films is increased compared to pure CdO and the band gap of Mn and Mn/Ni doped CdO should be larger than that of pure CdO. They also concluded that doped materials can lead to a change in the free electron density in the conduction band, which affects the position of the Fermi level and thus changes the band gap properties of metal oxides [32].

3.5 Spectroscopic ellipsometry analysis

The foundation of spectroscopic ellipsometry is the measurement of the material's response to polarized light reflection. ψ and Δ spectra are captured at every wavelength and angle of incidence in spectroscopic ellipsometer measurements. The following equation expresses the ψ and Δ parameters, which are related to the optical and structural characteristics of the sample and depend on the fresnel coefficients [33]:

$$\rho = tan\Psi\, e^{i\Delta} = R_p/R_s$$

In this equation, the complex reflection coefficients of light polarized vertically (s) and parallel (p) to the plane of incidence are denoted by the variables R_s and R_p in this equation, respectively. For the p- and s-polarized components, Δ represents phase shift between the incident and reflected waves, and ρ is the complex reflectance ratio. tanψ is the ratio of the reflection coefficient polarized parallel to the incidence plane to the reflection coefficient polarized perpendicular to the incident plane. For the studied spectral range of 300–1100 nm, the incidence angle of light employed for the measurements was 70°. Figure 8a, b displays the Δ and ψ values of pure CdO, CdO: B, CdO: Ga, and CdO: B-Ga thin films vs. wavelength. The Mean Squared Error (MSE) is used to assess the goodness of fit throughout the fitting process. The MSEs of the best fits are low enough (less than 30) to show that the model describes these thin film samples well. Pure CdO, CdO: B, CdO: Ga, and CdO: B-Ga thin films had MSE values of 4.195, 4.321, 3.264, and 4.464, respectively. The dielectric functions, optical constants, and absorption coefficients of the films were determined by Wang and co-workers using model fittings of the relative change in the polarization state of incident and reflected light (i.e. the amplitude ratio and phase difference spectra) obtained from SE measurements, as well as the measured spectra obtained from the as-grown CdO film at incident angles of 60°, 65°, 70°, and 75°.The results showed excellent fits with the models across the whole spectral range [34].

In order to appropriately build semiconductor devices, the dispersion of refractive indexes should be investigated. In many studies of integrated devices where the refractive index is crucial, such as in the design of filters, switches and modulators, it is important to understand the optical dispersion and other optical properties of the material. An optical medium's refractive index is a dimensionless quantity that describes how a beam travels through it [35]. The way fast-light travels through an object is determined by its refractive

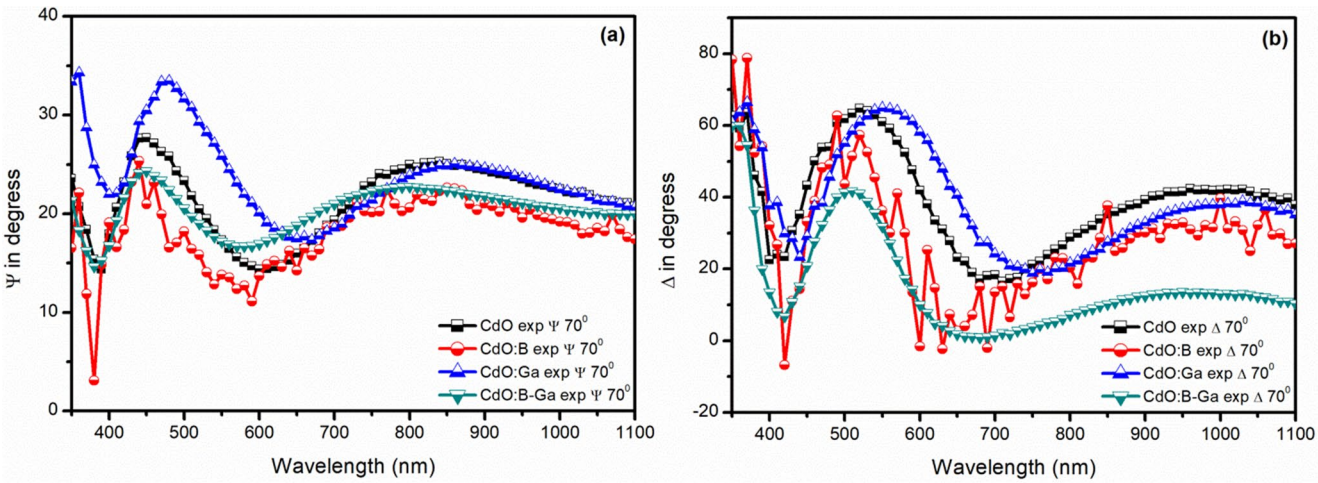

Fig. 8 Experimental results of ellipsometric data of pure and doped CdO thin films for **(a)** Psi (ψ), **(b)** Delta (Δ)

index. It is clear from Fig. 9(a) that the visible region's refractive index values for pure and doped CdO thin films range between 0.8 and 2. Upon searching the refractive indexes, it was found that Ga dopant's values were lower than those of the pure CdO thin film. The material's optical dispersion behavior is the cause of this drop in the refractive index value. Additionally, it can be observed that Ga and B-Ga dual doped CdO thin films have slightly lower refractive indices than pure and B doped CdO thin films. This may be due to the decreased electron polarization capacity of the B and Ga elements in the CdO structure.

The percentage of the beam lost as it travels through the material is measured by the extinction coefficient, which is connected to the substance's absorption property. Scattering and absorption per unit distance of the medium cause radiation loss [36]. Figure 9(b) shows that the extinction coefficient values for all semiconductor thin films ranged from 0.05 to 1.2, which was a good range for the absorber layer. Furthermore, the extinction coefficient decreased as a result of the B and Ga dopants especially after the wavelength of 700 nm. According to the literature conducted by R. A. Zargar et al., the refractive index values for TiO_2–CdO coated films increase as wavelength increases up to the band gap regime, after which it remains saturated and drops from 1.87 to 1.74 at 10% CdO content. This variation in the refractive index value is attributed to changes in crystallinity and increased film packing density. This demonstrates that the refractive index is dispersed appropriately within the band gap range. Additionally, the films' extinction coefficient (k) initially increased as wavelength grew; then, as wavelength increased alongside Cd doping in the band gap area, it began to decrease; finally, it remained nearly constant at higher wavelengths. The substitution of Cd atoms causes a local structural alteration that stimulates this shift of k and n in the band gap section. Their capacity to build optoelectronic devices is enhanced in the UV–visible range by smaller and bigger values of n and k, respectively [37]. M.H. Kabir and colleagues discovered that the refractive index values of Sr-doped CdO films first rise to a certain point before continuing to fall as the wavelength increases. This suggests that the refractivity behavior of all films is abnormal. Furthermore, it has been discovered that the total refractive index of CdO films rises as the concentration of Sr doping increases. This may be due to the surface of the films becoming rougher. The researchers concluded that the concentration of Sr doping considerably impacts refractive index of CdO films within the same spectral wavelength range. The same team also looked at how the extinction coefficient of undoped and Sr-doped CdO thin films changed with wavelength. All samples show a dramatic decline in extinction coefficient as wavelength increases. Furthermore, Sr-doped films have a higher extinction coefficient value than undoped films; that is, the extinction coefficient progressively rises as the Sr-doping concentration does. They also came to the conclusion that this extinction coefficient behavior shows that as the concentration of Sr-doping rises, so does the CdO films' ability to absorb light [38].

In general, dielectric constants depend heavily on the material's electrical structure and are directly related to the stated density of its band gap, which affects the electromagnetic radiation that travels through the material. The following relationships were used to calculate the imaginary and real values of the dielectric constants [39]:

$$\epsilon_1 = n^2 - k^2$$

$$\epsilon_2 = 2nk$$

The imaginary and real dielectric constant values of pure, B and Ga dual-doped CdO films were observed to rise with wavelength in Fig. 10 (a) and (b), which was consistent with the refractive index graphs. The wavelength range of

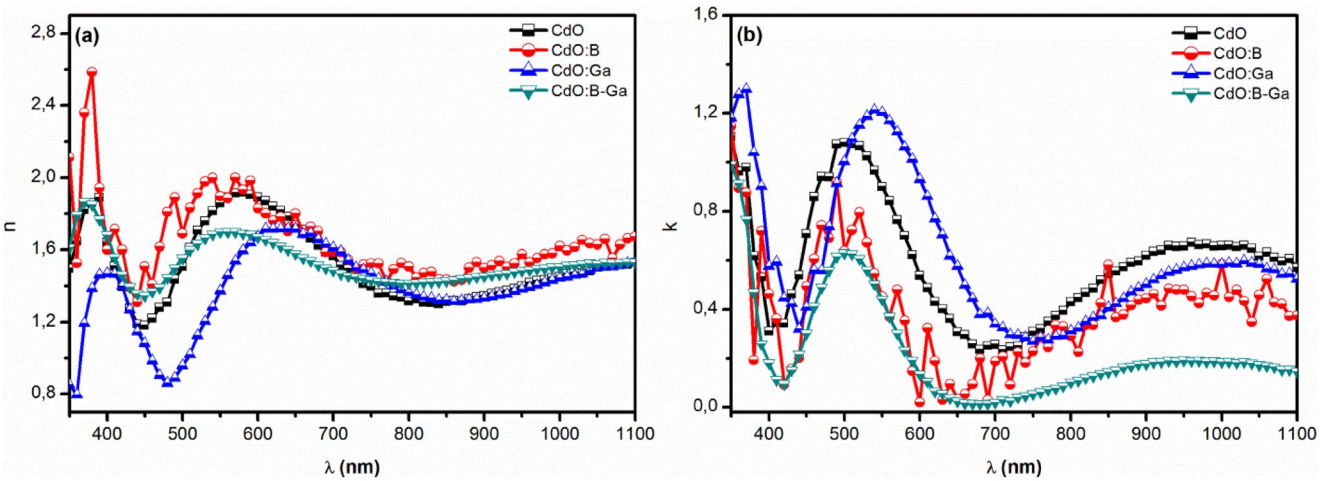

Fig. 9 The graph of **(a)** refractive index and **(b)** extinction coefficient of pure and doped CdO thin films

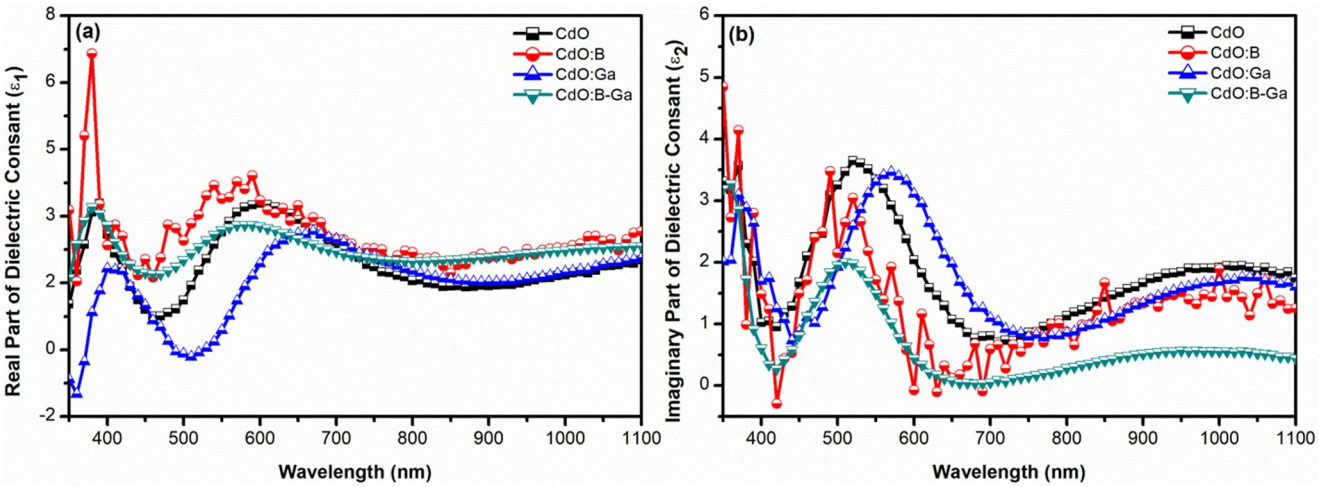

Fig. 10 Changes of **(a)** real and **(b)** imaginary part of dielectric constants as a function of wavelength for pure and doped CdO thin films

400–600 nm exhibits a sharper increase and decrease in real and imaginary dielectric constant values. It is also evident that the dielectric constants decreased as a result of the B and Ga dopant. The real and imaginary dielectric constant values for all nanostructured thin films also show significant variation in the visible region when the graphs are analyzed. It is evident that in every sample, the mean ϵ_1 values are greater than the ϵ_2 values. The state densities in the films' energy band gaps are connected to this discrepancy between the real and imaginary components. R.S. Ibrahim et al. examined how the real component of the dielectric constant varies with wavelength for both pure CdO and K-doped CdO thin films. It is shown that as the ratio of K doping is raised, ϵ_1 increases. Furthermore, increasing K doping in CdO results in a dramatic increase in the ϵ_1 parameter in the visible range, which is explained by the films' increased reflectance and decreased absorption [40]. V. Ganesh and his colleagues used the observed optical data in the 300–2400 nm range to compute the dielectric characteristics of the Tb-doped CdO thin films. They discovered that the wavelength of the incident light has a significant impact on the dielectric constant. Similar to the refractive index, the greatest values are seen in the infrared portion of the spectrum. Over the whole range shown in the figure, the impact of Tb doping on the dielectric constant is not consistent. They also came to the conclusion that Tb doping increases the observable range of the dielectric constant [41].

In applications involving optoelectronic devices, the energy loss function plays a significant role. It matters how much power is lost overall (volume and surface energy) via the dielectric. The dissipation factor (tan (δ)) represents the phase difference in materials caused by energy loss and is a valuable term in the evaluation of structure and flaws in materials [42]. Low dissipation factor values indicate the perfection of the dielectric as a desirable property. In a loss

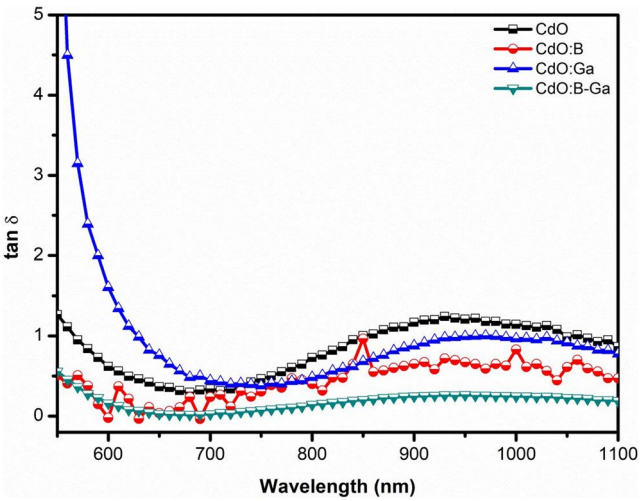

Fig. 11 Dissipation factor vs. photon wavelength for pure and doped CdO thin films

modulus system, the loss factor is correlated with the tan δ power loss rate, and tan δ depends on the real and imaginary parts of the dielectric constants in the manner described below [43].

$$tan\delta = \frac{\epsilon_2}{\epsilon_1}$$

The complex dielectric constant in this case is denoted by ϵ, which is made up of the real and imaginary components ϵ_1 and ϵ_2.

The wavelength vs. tan (δ) graph is displayed in Fig. 11. Pure and doped CdO thin films show a virtually constant dependence for all wavelength values in the graph, while Ga-doped CdO thin films show a high dependence between the around 600 nm wavelengths. This may be due to the abrupt drop in the absorption coefficient. M. Anitha et al.

investigated Zn-doped CdO thin films and found that the dissipation factor decreases with increasing wavelength. Furthermore, they demonstrated that the dissipation factor decreases rapidly between 450 and 500 nm, before remaining constant at longer wavelengths. They also reported that photon-electron interaction occurs in the thin films at shorter wavelengths [44]. The dissipation factor of fluorine-doped CdO thin films decreases with wavelength, according to research by M. Anitha and colleagues. Additionally, it is seen that the dissipation factor stays constant at longer wavelengths and drops off significantly between 450 and 500 nm. According to their findings, photon-electron interaction occurs in the thin-film region at shorter wavelengths [45].

4 Conclusion

In this study, it was aimed to obtain CdO films with pure and B, Ga and B-Ga dual-doped on ITO substrates by electrodeposition technique. The crystallinity size in all films varied depending on the calculation method. The structure deteriorated with the dual-doped B and Ga elements. A similar situation is also valid for the peak intensities. While the peak intensity increased in pure CdO, the peak intensity started to decrease with doping. This situation may be due to the difference in ionic radius between ions. When the SEM images of the obtained films were examined, it was seen that the film surfaces were formed in a smooth and homogeneous continuous structure without cracks, voids and pores and the p-Si substrates were well coated. Absorption and transmittance measurements of the films were taken in the 200–900 nm wavelength range. When the calculated E_g values of the CdO films were examined, it was seen that the E_g value changed with the doping element and the highest E_g value was obtained in the CdO: B-Ga, while the smallest E_g value was obtained in the pure CdO. The spectroscopic ellipsometry data demonstrate the dual doping effects on the optical characteristics of deposited thin films. Dopant components affect the deposited films' extinction coefficient, refractive index, real dielectric constant, imaginary dielectric constant, and dissipation factor. The studies carried out have shown that the amount and type of dopants have a significant effect on the structural, morphological and optical properties of the obtained films.

Author contributions EK: Writing-original draft, data curation, investigation EE: Methodology, writing-review and editing, conceptualization, visualization, validation.

Funding This work was funded by Bilecik Seyh Edebali University Scientific Research Coordination Unit (Project Number: TEZ-Y-2025-660).

Data Availability Data available on request from the authors.

Declarations

Competing interests The authors declare no competing interests.

References

1. S. Sivakumar, A. Venkatesan, P. Soundhirarajan, C.P. Khatiwada, Synthesis, characterizations and anti-bacterial activities of pure and Ag doped CdO nanoparticles by chemical precipitation method. Spectrochim. Acta A Mol. Biomol. Spectrosc. **136**, 1751–1759 (2015)
2. S.G. Ruvalcaba-Manzo, S.J. Castillo, M. Flores-Acosta, R. Ochoa-Landín, R. Ramírez-Bon, Study of optical, morphological, structural, and chemical properties of CdO thin films synthesized by thermal annealing transformation of $CdCO_3$ thin films. Opt. Mater. **132**, 112742 (2022)
3. K. Sirohi, S. Kumar, V. Singh, N. Chauhan, A. Vohra, Facile synthesis of CdO–ZnO nanocomposites for photocatalytic application in visible light. Arab. J. Sci. Eng. **49**(1), 273–284 (2024)
4. Z. Yang, P.F. Sun, X. Li, B. Gan, L. Wang, X. Song, H.D. Park, C.Y. Tang, A critical review on thin-film nanocomposite membranes with interlayered structure: mechanisms, recent developments, and environmental applications. Environ. Sci. Technol. **54**(24), 15563–15583 (2020)
5. K. Dhamodharan, R. Yuvakkumar, V. Thirumal, G. Ravi, M. Isacfranklin, S.A. Alharbi, T.A. Alahmadi, D. Velauthapillai, Effect of Nd^{3+} doping on CdO nanoparticles for supercapacitor applications. Ceram. Int. **47**(21), 30790–30796 (2021)
6. F. Unal, M.S. Kurt, S. Aktas, M. Kabaer, Synthesis and optoelectronic characterization of coronene/CdO self-powered photodiode. J. Mater. Sci. Mater. Electron. **33**(33), 25304–25317 (2022)
7. T. Prakash, D. Murugesan, K. Moulaee, G. Neri, S. Srimala, Synthesis, characterization, and gas sensing application of crumpled CdO sheets prepared in alkaline media. Mater. Res. Bull. **166**, 112339 (2023)
8. M.N. Le, P. Lee, S.H. Kang, K. Ahn, S.K. Park, J. Heo, M.G. Kim, Optimization of solution-processed amorphous cadmium gallium oxide for high-performance thin-film transistors. J. Mater. Chem. C **11**(22), 7433–7440 (2023)
9. A.A.A. Farag, A.M. Aboraia, H.E. Ali, V. Ganesh, H.H. Hegazy, A.V. Soldatov, H.Y. Zahran, Y. Khairy, I.S. Yahia, Structural investigation and optical enhancement characterization of nanostructured Ga-doped@ CdO/FTO films for photodiode applications. Opt. Mater. **110**, 110458 (2020)
10. K. Liu, Z. Li, X. Wu, Y. Fang, W. Zhou, J. Yang, Y. Sun, R. Niu, Z. Shao, L. Chen, R. Zhao, Y. Song, Impact of aluminum doping on nonlinear absorption and ultrafast carriers dynamics of Al: CdO thin films. Opt. Laser Technol. **157**, 108675 (2023)
11. S. Gupta, R. Lalwani, M. Gupta, P.K. Sahu, S. Onkarnath, Banerjee, Impact of dy ion on the structure and optoelectronic properties of CdO thin films: sol-gel spin coating method. Appl. Phys. A **131**(7), 561 (2025)
12. H.I. Hussein, A.H. Shaban, I.H. Khudayer, Enhancements of p-Si/CdO thin films solar cells with doping (Sb, Sn, Se). Energy Procedia **157**, 150–157 (2019)
13. N. Kumar, K. Arora, M. Kumar, Role of oxygen and Boron to control the duality behavior and thermal stability in Boron doped amorphous indium-zinc-oxide thin films. Semicond. Sci. Technol. **34**(5), 055004 (2019)
14. P. Sakthivel, S. Asaithambi, M. Karuppaiah, R. Yuvakkumar, Y. Hayakawa, G. Ravi, Improved optoelectronic properties of Gd

doped cadmium oxide thin films through optimized film thickness for alternative TCO applications. J. Alloys Compd. **820**, 153188 (2020)
15. V. Periasamy, P.N.N. Elumalai, S. Talebi, R.T. Subramaniam, R. Kasi, M. Iwamoto, Novel same-metal three electrode system for cyclic voltammetry studies. RSC Adv. **13**(9), 5744–5752 (2023)
16. E. Erdoğan, Production and characterization of electrodeposited cadmium sulfide semiconductor films with different Boron content. Cryst. Res. Technol. **59**(6), 2300353 (2024)
17. A. Begué, N. Cotón, R. Ranchal, Magnetic anisotropy evolution with Fe content in electrodeposited Ni_{100-x} Fe_x thin films. J. Mater. Chem. C **12**(27), 10104–10109 (2024)
18. P.A. Desai, A.A. Admuthe, S.D. Bhairannavar, R.H. Patil, V.S. Jamdade, S.G. Pawar, S.J. Rajoba, S.S. Kumbhar, S.H. Pisal, J.B. Thorat, I.A. Dhole, A study of NO_2 gas concentration on response of CdO thin films prepared by novel reflux method. J. Nano-Electron. Phys. **15**(5), 05033 (2023)
19. A. Mirzaei, E. Jamshidi, E. Morshedloo, S. Javanshir, F. Manteghi, Carrageenan assisted synthesis of morphological diversity of CdO and Cd $(OH)_2$ with high antibacterial activity. Mater. Res. Express. **8**(6), 065006 (2021)
20. M.A.H. Naeem, A.S.R. Ayon, M.M. Ali, M.R. Amin, M.H. Kabir, M.A. Sattar, S. Tabassum, M.N.H. Liton, Insights into the consequence of (Al–Zn) dual-doping on structural, morphological, and optoelectrical properties of CdO thin films. Heliyon **10**(4), e26545 (2024)
21. E. Erdoğan, A. Kiyak Yildirim, Synthesis of Zn-doped lead sulphide by electrodeposition: potential change on structural, morphological, and optical properties. J. Mater. Sci. Mater. Electron. **34**(10), 880 (2023)
22. E. Erdoğan, X-ray line-broadening study on sputtered InGaN semiconductor with evaluation of Williamson–Hall and size–strain plot methods. Indian J. Phys. **93**(10), 1313–1318 (2019)
23. M.K. Alam, M.S. Hossain, N.M. Bahadur, S. Ahmed, A comparative study in estimating of crystallite sizes of synthesized and natural hydroxyapatites using scherrer method, Williamson-Hall model, Size-Strain plot and Halder-Wagner method. J. Mol. Struct. **1306**, 137820 (2024)
24. W. Azzaoui, M. Medles, R. Miloua, A. Nakrela, A. Bouzidi, M. Khadraoui, A. Da Costa, M. Huvé, F. Bessuelle, R. Desfeux, Rietveld refinement combined with first-principles study of Zn and Al–Zn doped CdO thin films and their structural, optical and electrical characterisations. J. Mater. Sci. Mater. Electron. **34**(12), 1010 (2023)
25. M.H. Kabir, M. Hafiz, S.A. Urmi, M.J. Haque, M.M. Ali, M.S. Rahman, M.K.R. Khan, M.S. Rahman, Effect of Ga doping on microstructure, morphology, optical and electrical properties of spray deposited CdO thin films. Opt. Mater. **125**, 112123 (2022)
26. H. Cavusoglu, R. Aydin, B. Sahin, A comparative study on Cobalt and aluminum as a dual doping element for CdO films. Ceram. Int. **45**(1), 899–906 (2019)
27. R.J. Deokate, C.D. Lokhande, Liquefied petroleum gas sensing properties of sprayed nanocrystalline Ga-doped CdO thin films. Sensors Actuators B Chem. **193**, 89–94 (2014)
28. A.A. Ahmad, I.A. Aljarrah, A.A. Bani-Salameh, G. Toader, Optical, structural, electrical, and morphological properties of (Ga: B) co-doped cds thin films. J. Mater. Sci. Mater. Electron. **35**(26), 1730 (2024)
29. T. Noorunnisha, M. Suganya, M. Karthika, C. Kayathiri, K. Usharani, S. Balamurugan, V.S. Nagarethinam, A.R. Balu, (Zn+Co) co-doped CdO thin films with improved figure of merit values and ferromagnetic orderings with low squareness ratio well suited for optoelectronic devices and soft magnetic materials applications. Appl. Phys. A **126**, 1–9 (2020)
30. R. Halabi, A.M. Abdallah, M.I. Khalil, R. Awad, M. Mattar, Investigation of structural, optical, electrical, magnetic and antibacterial properties of (Mn and Sm) co-doped CdO nanostructures. Appl. Phys. A **129**(4), 307 (2023)
31. E. Erdogan, Coronene organic films: optical and spectral characteristics under annealing temperature influences. Surf. Rev. Lett. **28**(09), 2150081 (2021)
32. E. Gürbüz, R. Aydin, B. Şahin, A study of the influences of transition metal (Mn, Ni) co-doping on the morphological, structural and optical properties of nanostructured CdO films. J. Mater. Sci. Mater. Electron. **29**, 1823–1831 (2018)
33. S. Moradi, A. Nazari Setayesh, H. Sedghi, A comparative study on the structural and spectroscopic ellipsometry characterizations of (Co, Ni)-doped SnO2 nanostructured films spin-coated on glass substrates. Bull. Mater. Sci. **46**(1), 5 (2023)
34. Y. Wang, Y.Y. Chow, C.K.G. Kwok, Y.F. Leung, K.M. Yu, Effects of transition metal dopants (Mo and W) on electrical and optical properties of CdO thin films. J. Alloys Compd. **935**, 168116 (2023)
35. Z.R. Khan, M. Gandouzi, A.S. Alshammari, M. Bouzidi, M. Shkir, S. Alfaify, M. Mohamed, Structural, linear and nonlinear optical properties of Zn@ CdO nanostructured thin films: a quantitative comparison with DFT. J. Mater. Sci. Mater. Electron. **32**(13), 18304–18316 (2021)
36. B.S. Nagaraja, S.C. Gurumurthy, R. Bairy, K. Ramam, A. Rao, A systematic investigation on structural, electrical, linear and nonlinear optical properties of zn: CdO thin films for optoelectronic applications. Opt. Mater. **122**, 111669 (2021)
37. R.A. Zargar, M. Arora, S.A. Bhat, T. Mearaj, M.A. Manthrammel, M. Shkir, Growth of TiO2–CdO coated films: a brief study for optoelectronic applications. J. Phys. Chem. Solids **179**, 111390 (2023)
38. M.H. Kabir, A. Bhattacharjee, M.M. Islam, M.S. Rahman, M.S. Rahman, M.K.R. Khan, Effect of Sr doping on structural, morphological, optical and electrical properties of spray pyrolized CdO thin films. J. Mater. Sci. Mater. Electron. **32**(3), 3834–3842 (2021)
39. M.F. Hasaneen, M. Alzaid, M. Ezzeldian, A.A. El-Maaref, N.M.A. Hadia, Synthesis and physical properties of (CdO) 1-x (ZnO) x thin films obtained by electron beam evaporation for solar cell application. J. Non-Cryst. Solids **660**, 123552 (2025)
40. R.S. Ibrahim, A.A. Azab, T.A. Hameed, The effective role of potassium doping in improving the structural, morphological optical, and electrical properties of CdO thin film for optoelectronic application. Opt. Mater. **149**, 115100 (2024)
41. V. Ganesh, M.A. Manthrammel, M. Shkir, S. AlFaify, Investigation on physical properties of CdO thin films affected by Tb doping for optoelectronics. Appl. Phys. A **125**(4), 249 (2019)
42. M.G. Mulla, R.K. Pittala, Fabrication and physicochemical properties of nickel oxide (NiO) thin films. Ceram. Int. **51**(16), 22255–22265 (2025)
43. S. Demirezen, A. Dere, H.G. Çetinkaya, S.A. Mansour, F. Yakuphanoglu, Interface and dielectric properties of Al/p-Si diode by organic composite interlayer for MOS. J. Mater. Sci. Mater. Electron. **36**(14), 855 (2025)
44. M. Anitha, N. Anitha, K. Saravanakumar, I. Kulandaisamy, L. Amalraj, Effect of Zn doping on structural, morphological, optical and electrical properties of nebulized spray-deposited CdO thin films. Appl. Phys. A **124**(8), 561 (2018)
45. M. Anitha, K. Saravanakumar, N. Anitha, L. Amalraj, Influence of fluorine doped CdO thin films by an simplified spray pyrolysis technique using nebulizer. Opt. Quantum Electron. **51**(6), 187 (2019)